

Quantum dot origin of luminescence in InGaN-GaN structures

I. L. Krestnikov,* N. N. Ledentsov,* A. Hoffmann, and D. Bimberg

Institut für Festkörperphysik, Technische Universität Berlin, Hardenbergstrasse 36, 10623, Berlin, Germany

A. V. Sakharov, W. V. Lundin, A. F. Tsatsul'nikov, A. S. Usikov, and Zh. I. Alferov

A.F. Ioffe Physical-Technical Institute of Russian Academy of Sciences, Politekhnicheskaya 26, 194021, St. Petersburg, Russia

Yu. G. Musikhin* and D. Gerthsen

Laboratorium für Elektronenmikroskopie, Universität (TH) Karlsruhe, Kaiserstrasse 12, D-76128 Karlsruhe, Germany

(Received 17 April 2002; revised manuscript received 5 July 2002; published 4 October 2002)

We report on resonant photoluminescence (PL) of InGaN inclusions in a GaN matrix. The structures were grown on sapphire substrates using metal-organic chemical vapor deposition. Nonresonant pulsed excitation results in a broad PL peak, while resonant excitation into the nonresonant PL intensity maximum results in an evolution of a sharp resonant PL peak, having a spectral shape defined by the excitation laser pulse and a radiative decay time close to that revealed for PL under nonresonant excitation. Observation of a resonantly excited narrow PL line gives clear proof of the quantum dot nature of luminescence in InGaN-GaN samples. PL decay demonstrates strongly nonexponential behavior evidencing coexistence of quantum dots having similar ground-state transition energy, but very different electron-hole wave-function overlap.

DOI: 10.1103/PhysRevB.66.155310

PACS number(s): 78.67.Hc, 73.21.La, 78.47.+p, 78.55.Cr

There exists a continuous interest in understanding basic optical properties of GaN-based structures and lasers based thereupon.¹⁻⁴ Numerous investigations have been carried out to clarify the origin of luminescence and laser gain in InGaN-based structures (see, e.g., Ref. 5, and references therein). However up to now, there is still no clear picture of the basic radiative recombination processes in InGaN-based structures. Some researchers⁶⁻⁸ proposed that InGaN insertions represent ultradense ($> 10^{11} \text{ cm}^{-2}$) arrays of quantum dots (QD's). These QD's are claimed to be responsible for good luminescence properties of InGaN insertions,² as they suppress carrier diffusion towards various defects and were claimed to be crucial for lasing in InGaN-based injection structures.⁹ Previously, we stressed that, as in QD structures, the maximum modal gain is directly proportional to the volume density of QD's,¹⁰ and a maximum modal gain of about 10^5 cm^{-1} may be realized for wide-gap QD's having a density of 10^{18} cm^{-3} and a density-of-states broadening of a few tens of meV.^{7,11} This opens unique possibilities for device applications, particularly, for lasers. As opposite, completely different sizes and densities of QD's have been proposed in the literature for samples, grown under similar or different growth conditions, ranging from 3–5 nm (Refs. 3, 6, 7, 9, 12, and 13) to 20–30 nm.¹⁴ Sharp lines due to single QD's were revealed recently in InGaN samples with large (20 nm) InGaN islands, however, the number of these lines in the spectrum was small and the integrated intensity was weak with respect to the intense PL continuous background.¹⁴ The origin of this background was not identified.

One must also underline that there exists a conflicting set of optical data, which allowed many researchers to conclude that photoluminescence (PL) properties of wurtzite InGaN insertions may be explained only by quantum-well-like material distribution.^{4,15,16} Indeed, many groups reported a long-wavelength shift of InGaN PL after nonresonant excitation accompanied by a significant increase in the PL decay

time.¹⁷⁻²⁰ Takeuchi *et al.*²¹ observed a blueshift of the high-energy PL with increasing continuous-wave excitation density. In both cases, screening of piezoelectric potential separating electrons and holes in a quantum well (QW) at high excitation densities was proposed to be responsible for the above effects. Indeed, studies in GaN-based structures have shown that the shift of the transition energy due to a quantum confined Stark effect caused by piezoelectric potential may play an important role in the case of thick QW's (Refs. 22 and 23) or QD's.²⁴⁻²⁶ Opposite to QW's no further population of the QD is possible in the case of a photon having exactly the same energy, after the first exciton is created in a QD.²⁷ No screening of piezoelectric charge is thus possible with excitation density increase. This is opposite to the QW case, where a continuum of states exists, and a lot of electron-hole pairs can be generated in the same QW with an excitation density increase. This increase, in turn, should cause the PL high-energy shift with excitation density to increase, and, consequently, a long-wavelength energy shift upon depopulation of the QW by radiative or nonradiative recombination should occur. Lack of similar shift may evidence the true QD nature for the radiative states responsible for the maximum PL intensity. If so, a PL shift after the excitation pulse under nonresonant excitation also can be explained by depopulation of the QD density of states, or by a dependence of the radiative lifetime on the QD size. The radiative lifetime can be written as²⁸

$$\frac{1}{\tau_{\text{rad}}} = \frac{3}{8} \frac{e}{\hbar c} \sqrt{\epsilon} \omega \left(\frac{P}{\hbar c} \right)^2 I, \quad (1)$$

where ω is photon frequency, ϵ the dielectric susceptibility of the host medium, and P the optical interband matrix element describing the contribution of the Bloch functions.²⁸ Here we additionally included a term I , which characterizes

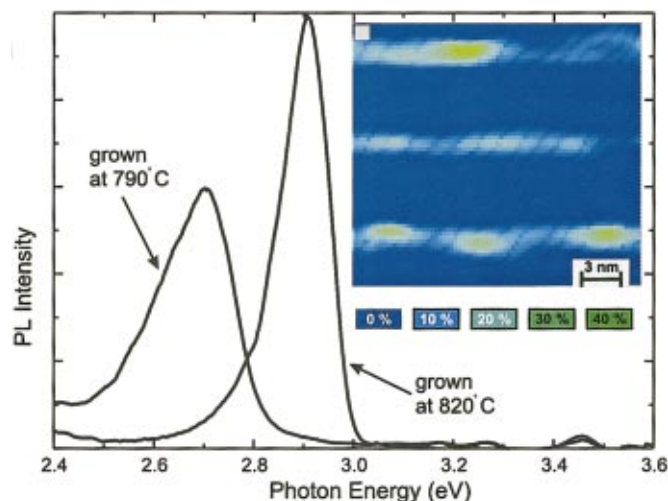


FIG. 1. (Color) Time-integrated photoluminescence (PL) spectra of samples grown at 790 °C and 820 °C measured at excitation wavelength of 291 nm. Inset shows a color-coded map of the local indium content in the structure grown at 820 °C.

the overlap integral between the electron and the hole wave functions, which was assumed to be unity in Ref. 28 for simplicity.

Previously, we studied structural and optical properties of InGa_N-Ga_N structures and proposed that optical properties of our structures are completely governed by QD's.^{7,8,29} We observed that InGa_N insertions grown in typical growth conditions represent dense arrays of InN-rich nanodomains with size (3–5 nm) and density (10^{11} – 10^{12} cm⁻²) strongly affected by growth conditions.³⁰ Ultrahigh modal gain related to ultradense arrays of QD's resulting in lifting the *k*-selection rule for direct exciton recombination was proposed to explain the possibility to reach maximum modal gain values of 10⁵ cm⁻¹ in multisheet InGa_N-Ga_N lasers³¹ necessary to achieve surface lasing in low finesse cavities. In this paper we confirm the above proposal and present direct evidence of QD's responsible for the major part of the broad PL spectrum at high excitation densities in time-resolved (TR) PL studies.

The structures investigated in this paper were grown on a (0001) *c*-plane sapphire substrate by metal-organic chemical vapor deposition. The structure consists of a 2.5-μm Ga_N buffer layer, with an active region of a 10-period InGa_N/Ga_N superlattice and a 0.07-μm Ga_N cap layer. Formation of a 3-nm InGa_N/7-nm Ga_N superlattice was achieved by periodic substrate temperature variation from 790 °C to 885 °C and from 820 °C to 915 °C for two different structures. The TR PL was measured at 2 K under tunable dye laser excitation with a repetition rate of 3.79 MHz at wavelengths of 291 (4.26) and 424 nm (2.925 eV) with excitation density of 600 W/cm². Registration of TR PL was performed using a fast response multichannel photomultiplier (rise time is less than 5 and decay time is less than 30 ps). The high-resolution transmission-electron microscopy (HRTEM) studies were carried out using a Philips CM20 FEG/ST electron microscope operating at 200 kV.

In Fig. 1 we show time-integrated spectra of our samples

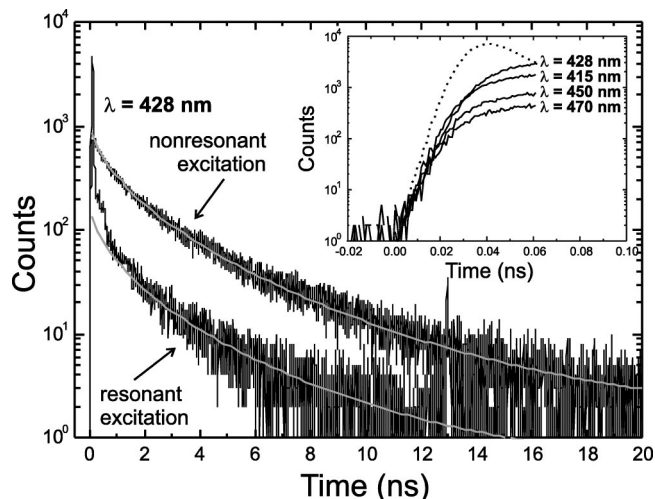


FIG. 2. Time-resolved PL for structure grown at 820 °C under nonresonant and resonant excitation at 428 nm. Gray lines correspond to the fitting by Eq. (2). Inset shows time-resolved PL under nonresonant excitation at different registration wavelengths. Dotted line presents resolution of the registration system.

measured at an excitation wavelength of 291 nm. Since the active regions were grown at different substrate temperatures and the indium evaporation rate strongly depends on the substrate temperatures, the samples have different average indium concentrations in the active regions. It leads to the different PL peak energies related for two samples. The DALI (Ref. 32) processed HRTEM image of the sample grown at higher temperature is shown in the inset of Fig. 1. An array of In-rich nanodomains having a 3-nm lateral size is revealed. The dot shape was similar for both samples while the dot density and average In composition in the QD's were lower for the sample grown at higher temperature extensively studied in this work. More information on structural properties of the InGa_N nanodomains is given in Ref. 30. Maximum In content inside the nanodomain was at least two times higher than the average content of the QW (18% and 23% for structures grown at higher and lower temperatures, respectively). There exists a spread in values of size and content of InGa_N nanodomains. Significant size and composition dispersion of the InGa_N nanodomains is responsible for the broadening of the PL spectrum up to about 200 meV.

According to our nonresonant time-resolved PL studies the PL emission decay demonstrates a nonexponential behavior with gradual decrease in the PL decay rate with time (see Fig. 2). The PL intensity decay behavior $I(t)$ was well fitted by the stretched exponent:

$$I(t) = I_0 \exp[-(t/\tau^*)^\beta], \quad (2)$$

where β and τ^* are the stretching parameter and time constant, respectively. The stretched exponential behavior is usually observed in PL studies of heavily disordered media.³³ This behavior was also revealed for InGa_N/Ga_N structures in a number of papers.^{34–36} This dependence was mostly attributed to a gradual increase in the lifetime with gradual non-equilibrium carrier depopulation of the quantum wells, caus-

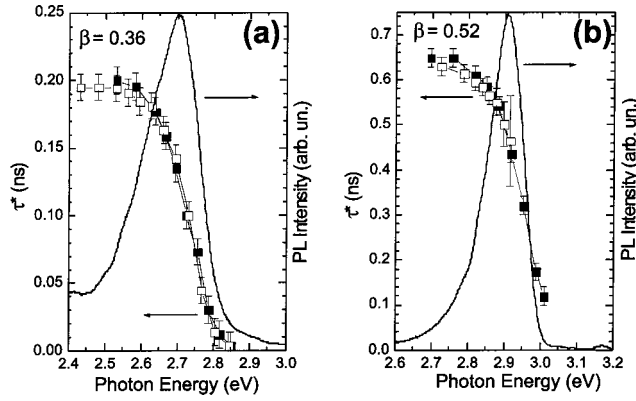


FIG. 3. Dependencies of time constant vs registration wavelength for samples grown at 790 °C (a) and 820 °C (b). Filled squares correspond to the excitation wavelength of 291 nm, while open squares to 424 nm. Time-integrated PL spectra are presented by solid lines.

ing a reduced screening of the piezoelectric charge and lower electron-hole overlap. An alternative explanation can be related to size, shape, and composition dispersion of InGaN quantum dots, where QD's having similar transition energies have different electron-hole wave-function overlap. Radiative decay of QD's with reduced overlap dominates at large time delays after the excitation pulse. Since the size, composition, and the shape of the QDs, as well as their uniformity, strongly depend on growth conditions, one must expect the corresponding changes for samples grown at different temperatures. The stretched parameters (β) are 0.35 and 0.5 for structures grown at lower and higher temperatures, consequently, and they are almost independent of excitation and detection wavelength. As it follows from Ref. 30 the confinement potential depth for QD's formed at lower temperatures is stronger, while the size is comparable. This defines the higher overlap of electron and hole wave functions. Consequently, a shorter-time constant for the structure grown at lower temperature is found. As can be clearly seen from Fig. 3 the time constants strongly decrease on the short-wavelength side of the PL spectrum with characteristic energy of about 40 meV for both structures grown at 790 °C and 820 °C. Such behavior may be expected for systems where there exists an efficient energy relaxation of carriers from higher- to lower-energy states.³⁷ Shortening of the PL decay time along the PL contour when moving towards the high-energy side of the spectrum can be attributed to carrier hopping through the band of localized states in a QW, which have much lower density with respect to the quantum-well continuum.^{38,39} This behavior is then accompanied by slow time evolution of the long-wavelength component of the spectra, since the electrons and the holes need time to reach the localized states, the hopping time is long, and, additionally, electrons and holes need to find each other in the same localization potential. As is opposite in our case, the PL signal appears with an onset time faster than 5 ps, which is our time resolution (see inset of Fig. 2), and a hopping model can hardly be applied. We rather may attribute the observed shortening of the decay time to a population of higher-lying excited QD states accompanied by their fast en-

ergy transfer to the ground states. We note that after the excitation pulse the PL peak maximum gradually shifts towards the longer-wavelength side of the spectrum. This effect may be explained by longer radiative decay times for larger QD's [Eq. (1)]. An alternative, "quantum-well" explanation may refer to spectral diffusion and piezoelectric screening effects.

The key experiment, which can clarify unambiguously the nature of processes involved, is the resonant excitation of PL. In the case when the QW is excited, the carrier transfer towards the states having a lower energy occurs, accompanied by fast evolution of the thermalized luminescence peak. In the case of wurtzite-type strained quantum wells having a strong builtin piezoelectric field, reduced carrier concentration upon the radiative recombination of nonequilibrium carriers must result in reduced screening of the piezoelectric potential, further shifting PL towards the longer-wavelength side of the spectra and strongly increasing the PL decay time. Neither of these effects was revealed in our case.

In our work we compared below the GaN barrier (excitation energy of 2.925 eV) resonant and nonresonant excitation for the two samples studied. For the sample grown at 790 °C the excitation energy was at significantly higher photon energies than the PL peak maximum. In this case, the PL peak had the same shape as the case of the above barrier excitation at 4.26 eV. Oppositely, for the sample grown at 820 °C, the excitation wavelength exactly matches the PL peak maximum. A completely different behavior is revealed in this case.

In Fig. 4(a) we present time/wavelength plots of PL for nonresonant and resonant [Fig. 4(b)] excitation. In the case of nonresonant excitation one can see an inhomogeneously broadened PL peak which gradually decays with time and shifts towards the lower-energy side of the spectrum. After the resonant excitation pulse (white color) the shape of the PL spectrum is completely different. Most of the PL intensity, after the exciting laser light is gone, exactly resembles the spectral shape of the excitation source; even the decay time of this signal corresponds to the radiative decay times after nonresonant excitation. This unambiguously evidences the QD origin of the signal. The PL peak position does not shift in time and no spectral broadening was observed (Fig. 4). This may rule out any importance of the spectral diffusion and gradual weakening of the piezoelectric screening with carrier depopulation, which both should take place in QW samples. The observed behavior fits exactly the behavior of resonantly excited QD's having a delta-function-like density of state⁴⁰ and no exciton or carrier transfer at low temperatures. The fact that the observed behavior is typical for the central part of the PL peak at high excitation densities, where lasing occurs, stresses the importance of QD's in the lasing process. In our previous paper³¹ we found that the laser generation at room temperature occurs at a low-energy side of the broad PL peak. This means that the localized states are responsible for the lasing process even at high temperatures.

An additional weak shoulder is revealed on the longer-wavelength side of the PL spectrum. The shift of excitation wavelength to low energy results in a strong suppression of the relative intensity of the long-wavelength shoulder. This

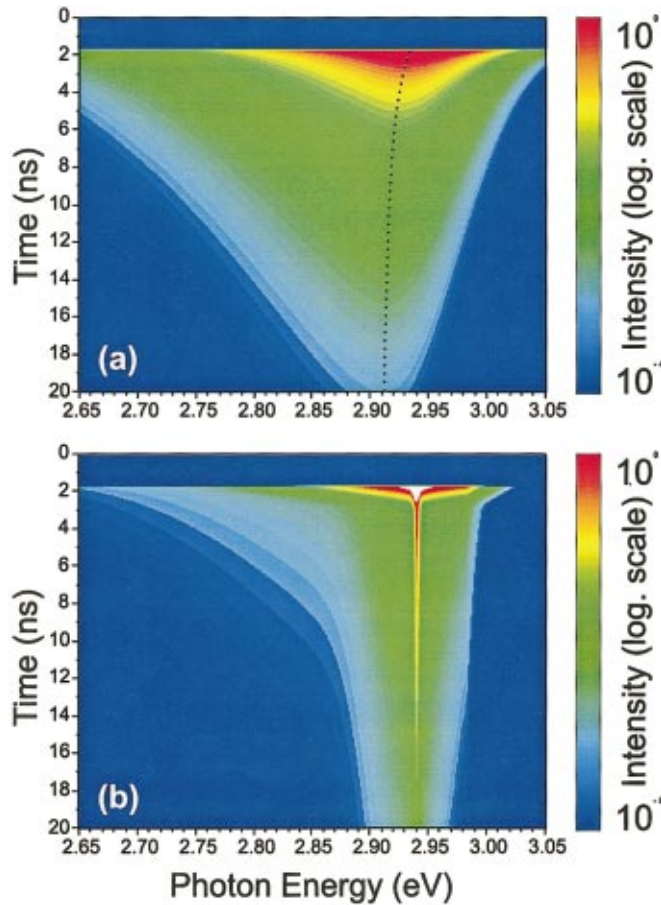


FIG. 4. (Color) Time/wavelength plots of PL for nonresonant (a) and resonant (b) excitations for sample grown at 820 °C. White spot corresponds to the scattered laser light.

shoulder transforms into a well-resolved peak, if the resonant PL background is subtracted. The procedure of subtracting resonant PL was based on independent measurement of the intensity of the scattered laser light. It was found that the resonant component of the PL in time-resolved experiments fits exactly the intensity profile of the scattered laser light except for the longer-wavelength part of the PL spectra. Thus, this “long-wavelength” part could be precisely defined by normalizing the scattered light intensity profile to the resonant PL intensity maximum with further subtraction of this resonant component. This procedure does not include any arbitrary parameters and is straightforward. The shoulder appears on a time scale < 5 ps after the laser pulse and can be attributed to the fast energy transport from the QD exciton excited state towards its ground state. Due to the significant

size dispersion of QD's, larger QD's may have an excited-state energy which fits the ground-state energy of the major QD's. A maximum of this PL emission is shifted from the resonant PL peak by about 40–50 meV towards the lower energies giving an estimate for energy splitting between the QD ground state and the first excited state. Applying the simplest model of spherical nanodomains with infinite barriers,⁴¹ the difference between the first excited and ground states are given by the following equation:

$$\Delta E = \frac{3}{2m_h} \left(\frac{\pi\hbar}{R} \right)^2 - 0.248E_{Ry}^*, \quad (3)$$

where m_h is the hole effective mass, R the nanodomain radius, and E_{Ry}^* the exciton binding energy. Assuming the hole effective mass of moderate In composition to be $1.0m_0$ and nanodomain radius to be 2.5 nm we obtained from Eq. (3) value of 70 meV which, generally, fits well to the experimental value, assuming some uncertainty in size and composition profile of the QD's. The first excited state in this model is the transition between the first heavy hole and the ground electron state. This transition is partially allowed due to the different confinement potentials for electrons and holes in a QD.²⁵ The latter statement is particularly true for wurtzite-type QD's, having a significant contribution of a piezoelectric potential. The value of the splitting between the QD ground state and the first excited state is in good agreement with the value of characteristic photon energy on the high-energy side of the nonresonant PL spectrum, which marks a fast decreasing of τ^* .

In conclusion, we believe that our results unambiguously demonstrate a quantum dot origin of InGaN luminescence in our samples. Formation of the InGaN nanodomains revealed in electron microscopy studies agrees well with the PL trends. No signs of spectral diffusion or piezoelectric potential screening were revealed in our structures. The nonexponential decay of the resonant PL evidences coexistence of QD's having the same ground-state transition energy, but different electron-hole wave-function overlaps due to shape, size, and composition nonuniformity. Resonant PL studies may thus serve as an important tool to investigate in detail the probability of radiative recombination, and its dispersion in highly disordered QD systems.

This work was supported by the DFG Graduiertenkolleg “Collective Phenomena in Solids,” the RFBR, and the grant “NATO for Peace.” I.L.K. thanks the Alexander von Humboldt Foundation. N.N.L. acknowledges a DAAD Guest Professorship and an equipment donation from the Alexander von Humboldt Foundation.

*On leave from A.F. Ioffe Physical-Technical Institute, St. Petersburg, Russia.

¹S. Nakamura, *Science* **281**, 956 (1998).

²K. P. O'Donnell, R. W. Martin, and P. G. Middleton, *Phys. Rev. Lett.* **82**, 237 (1999).

³H. Chen, R. M. Feenstra, J. E. Northrup, T. Zywiets, and J. Neugebauer, *Phys. Rev. Lett.* **85**, 1902 (2000).

⁴C.-K. Sun, J.-C. Liang, and X.-Y. Yu, *Phys. Rev. Lett.* **84**, 179 (2000).

⁵H. Morkoc, *Nitride Semiconductors and Device* (Springer-Verlag, Berlin, 1999).

⁶S. Chichibu, T. Azuhata, T. Sota, and S. Nakamura, *Appl. Phys. Lett.* **69**, 4188 (1996).

⁷N. N. Ledentsov, Zh. I. Alferov, I. L. Krestnikov, W. V. Lundin,

- A. V. Sakharov, I. P. Soshnikov, A. F. Tsatsul'nikov, D. Bimberg, and A. Hoffmann, *Comp. Semicond.* **5**(9), 61 (1999).
- ⁸A. V. Sakharov, W. V. Lundin, I. L. Krestnikov, V. A. Semenov, A. S. Usikov, A. F. Tsatsul'nikov, Yu. G. Musikhin, M. V. Baidakova, Zh. I. Alferov, N. N. Ledentsov, J. Holst, A. Hoffmann, D. Bimberg, I. P. Soshnikov, and D. Gerthsen, *Phys. Status Solidi B* **216**, 435 (1999).
- ⁹Y. Narukawa, Y. Kawakami, M. Funato, S. Fujita, S. Fujita, and S. Nakamura, *Appl. Phys. Lett.* **70**, 981 (1997).
- ¹⁰M. Asada, M. Miyamoto, and Y. Suematsu, *IEEE J. Quantum Electron.* **QE-22**, 1915 (1986).
- ¹¹D. Bimberg, M. Grundmann, and N. N. Ledentsov, *Quantum Dot Heterostructures* (Wiley, New York, 1999).
- ¹²I. P. Soshnikov, V. V. Lundin, A. S. Usikov, I. P. Kalmykova, N. N. Ledentsov, A. Rosenauer, B. Neubauer, and D. Gerthsen, *Semiconductors* **34**, 621 (2000).
- ¹³L. Nistor, H. Bender, A. Vantomme, M. F. Wu, J. Van Landuyt, K. P. O'Donnell, R. Martin, K. Jacobs, and I. Moerman, *Appl. Phys. Lett.* **77**, 507 (2000).
- ¹⁴O. Moriwaki, T. Someya, K. Tachibana, S. Ishida, and Y. Arakawa, *Appl. Phys. Lett.* **76**, 2361 (2000).
- ¹⁵C. Wetzel, T. Takeuchi, H. Amano, and I. Akasaki, *J. Appl. Phys.* **85**, 3786 (1999).
- ¹⁶L.-H. Peng, C.-W. Chuang, and L.-H. Lou, *Appl. Phys. Lett.* **74**, 795 (1999).
- ¹⁷H. Yu, H. Htoon, A. deLozanne, C. K. Shih, P. A. Grudowski, R. D. Dupuis, K. Zeng, R. Mair, J. Y. Lin, and H. X. Jiang, *J. Vac. Sci. Technol. B* **16**, 2215 (1998).
- ¹⁸H. Kudo, H. Ishibashi, R. Zheng, Y. Yamada, and T. Taguchi, *Appl. Phys. Lett.* **76**, 1546 (2000).
- ¹⁹S. Chichibu, T. Azuhata, T. Sota, and S. Nakamura, *Appl. Phys. Lett.* **69**, 4188 (1996).
- ²⁰J. Li, K. B. Nam, K. H. Kim, J. Y. Lin, and H. X. Jiang, *Appl. Phys. Lett.* **78**, 61 (2001).
- ²¹T. Takeuchi, Sh. Sota, M. Katsuragawa, M. Komori, H. Takeuchi, H. Amano, I. Akasaki, *Jpn. J. Appl. Phys., Part 2* **36**, L382 (1997).
- ²²F. Bernardini, V. Firoentini, and D. Vanderbilt, *Phys. Rev. Lett.* **79**, 3958 (1997).
- ²³Ch. Wetzel, T. Takeuchi, H. Amano, and I. Akasaki, *Jpn. J. Appl. Phys., Part 2* **38**, L163 (1999).
- ²⁴A. D. Andreev and E. P. O'Reilly, *Phys. Rev. B* **62**, 15 851 (2000).
- ²⁵O. Stier, M. Grundmann, and D. Bimberg, *Phys. Rev. B* **59**, 5688 (1999).
- ²⁶S. Sanguinetti, M. Gurioli, E. Grilli, M. Guzzi, and M. Henini, *Appl. Phys. Lett.* **77**, 1982 (2000).
- ²⁷Creation of biexcitons via resonant excitation of QD's is also possible since biexciton and exciton states may be degenerated in energy for particular QD shapes and compositions. We note, however, that there is no reason to expect that this degeneracy exists for all types of QD's having the same ground-state transition energy. As we study QD's of various shapes and compositions even under the resonant excitation conditions, this coincidence may be expected only for a fraction of QD's. As the possible coexistence of degenerate biexciton and exciton states does not principally change our argumentation, we restrict our discussion at that point to just mentioning the general possibility of this effect.
- ²⁸L. V. Asryan and R. A. Suris, *Semicond. Sci. Technol.* **11**, 554 (1996).
- ²⁹I. L. Krestnikov, N. N. Ledentsov, A. Hoffmann, and D. Bimberg, *Phys. Status Solidi A* **183**, 207 (2001).
- ³⁰Yu. G. Musikhin, D. Gerthsen, D. A. Bedarev, N. A. Bert, W. V. Lundin, A. F. Tsatsul'nikov, A. V. Sakharov, A. S. Usikov, I. L. Krestnikov, N. N. Ledentsov, A. Hoffmann, and D. Bimberg, *Appl. Phys. Lett.* **80**, 2099 (2002).
- ³¹I. L. Krestnikov, W. V. Lundin, A. V. Sakharov, V. A. Semenov, A. S. Usikov, A. F. Tsatsul'nikov, Zh. I. Alferov, N. N. Ledentsov, A. Hoffmann, and D. Bimberg, *Appl. Phys. Lett.* **75**, 1192 (1999).
- ³²A. Rosenauer, S. Kaiser, T. Reisinger, J. Zweik, W. Gebhard, and D. Gerthsen, *Optik (Stuttgart)* **102**, 63 (1996).
- ³³H. Scher, M. F. Shlesinger, and J. T. Bender, *Phys. Today* **26**, 24 (1991).
- ³⁴M. Pophristic, F. H. Long, C. Tran, I. T. Ferguson, and R. F. Karliceck, Jr., *Appl. Phys. Lett.* **73**, 3550 (1998).
- ³⁵M. Pophristic, F. H. Long, C. Tran, I. T. Ferguson, and R. F. Karliceck, Jr., *J. Appl. Phys.* **86**, 1114 (1999).
- ³⁶A. Kaschner, J. Holst, U. von Gfug, A. Hoffmann, F. Bertram, T. Riemann, D. Rudloff, P. Fischer, J. Christen, R. Averbek, and H. Riechert, *MRS Internet J. Nitride Semicond. Res.* **5S1**, W11.34 (2000).
- ³⁷C. Gourdon and P. Lavallard, *Phys. Status Solidi B* **153**, 641 (1989).
- ³⁸Y. Narukawa, Y. Kawakami, S. Fujita, and S. Nakamura, *Phys. Rev. B* **55**, R1938 (1997).
- ³⁹L. E. Golub, S. V. Ivanov, E. L. Ivchenko, T. V. Shubina, A. A. Toropov, J. P. Bergman, G. R. Pozina, B. Monemar, and M. Willander, *Phys. Status Solidi B* **205**, 203 (1998).
- ⁴⁰M. Paillard, X. Marie, E. Vanelle, T. Amand, V. K. Kalevich, A. R. Kovsh, A. E. Zhukov, and V. M. Ustinov, *Appl. Phys. Lett.* **76**, 76 (2000).
- ⁴¹Y. Kayanuma, *Phys. Rev. B* **38**, 9797 (1988).